Amino Acids (2012) 43:1779–1790
DOI 10.1007/s00726-012-1262-6

ORIGINAL ARTICLE

Novel emissive bio-inspired non-proteinogenic coumarin-alanine amino acid: fluorescent probe for polyfunctional systems

Elisabete Oliveira · José Luis Capelo · João Carlos Lima · Carlos Lodeiro

Received: 27 October 2011 / Accepted: 29 February 2012 / Published online: 13 March 2012

Abstract Two new bio-inspired non-proteinogenic compounds **L1** and **L2**, containing coumarin and/or acridine chromophores and bearing as spacer an alanine amino acid were successfully synthesized and fully characterized by elemental analysis, ^{1}H and ^{13}C NMR, infrared spectroscopy (KBr discs), melting point, ESI-TOF (electrospray ionization-time of flight-mass), UV–vis absorption and emission spectroscopy, fluorescence quantum yields and lifetime measurements. A relative fluorescence quantum yield of 0.02 was determined for both compounds. In **L2** the presence of an intramolecular energy transfer from the coumarin to the acridine unit was observed. **L1** and **L2** are quite sensitive to the basicity of the environment. At alkaline values both compounds show a strong quenching in the fluorescence emission, attributed to the photoinduced electron transfer (PET). However, both deprotonated forms recover the emission with the addition of Zn^{2+}, Cd^{2+} and Al^{3+} metal ions. As multifunctional emissive probes, the titration of **L1** and **L2** with lanthanides (III), Eu^{3+} and Tb^{3+} was also explored as new visible bio-probes in the absence and in the presence of liposomes. In a liposomal environment a lower energy transfer was observed.

Keywords Alanine · Coumarin · Acridine · Liposomes · Lanthanide(III) · Transition metals

E. Oliveira (✉) · J. L. Capelo · C. Lodeiro (✉)
BIOSCOPE Group, Physical-Chemistry Department,
Faculty of Science, Ourense Campus, University of Vigo,
32004 Ourense, Spain
e-mail: e.oliveira@uvigo.es

C. Lodeiro
e-mail: clodeiro@uvigo.es

E. Oliveira
Veterinary Science Department (CECAV),
University of Trás-os-Montes and Alto Douro,
5001-801 Vila Real, Portugal

J. L. Capelo · J. C. Lima · C. Lodeiro
REQUIMTE/CQFB, Chemistry Department,
Faculty of Science and Technology, University Nova of Lisbon,
2829-516 Monte de Caparica, Portugal

Introduction

The design of new bio-inspired compounds (Lodeiro et al. 2010; Pazos et al. 2009) containing amino acid units (Costa et al. 2008; Oliveira et al. 2012a), peptides (Oliveira et al. 2011a, b), neurotransmitters (Oliveira et al. 2012b) or other biological molecules as receptors, and bearing fluorescent dyes is up to now an area of great development due to their huge potential applications in biological and environmental fields. A bio-inspired chemosensor has a similar structure to a classical chemosensor, but in this case, the receptor is formed by an amino acid (natural or synthetic) or by a peptide chain (Lodeiro et al. 2010).

The insertion of amino acids in the backbone of synthetic polymers can lead us to macromolecules containing biomimetic characteristics, with a specific structure and biological properties.

Their properties such as luminescence, conducting ability, higher thermal stability and metal ions or other analyte recognition, can be modified by synthetic manipulation at the amino acids side chain. Amino acids and peptides contain sites available for metal binding and recognition, making them good biosensors for metal detection in solution and in solid state (Costa et al. 2007). Peptides and proteins do not have fluorescent properties strong enough to be useful as intrinsic fluorescence chemosensor for sensing in the environment. So, their

conjugation with emissive fluorophores can enhance their properties, for sensing and developing fluorescence peptide sensors.

Classically, the most common fluorophores used in molecular chemosensors, anthracene (Tamayo et al. 2005; Kubo and Mori 2005), pyrene (Yang et al. 2001; Lodeiro et al. 2006), benzoxazol (Costa et al. 2007, 2008), have short emission wavelengths which fit perfectly for abiotic analysis, but when we cross for in vivo applications the fluorophores used must be visible excited. Coumarin (Lim and Bruchner 2004; Oliveira et al. 2011a, b; Lu et al. 2007), acridine (Lee et al. 2008), fluorescein (Burdette et al. 2001; Nolan et al. 2006) and rhodamine (Soh et al. 2007; Ko et al. 2006; Zhang et al. 2009) dyes are often applied in biological studies. As stated above, the fluorophores have an important role, and then its properties are extremely important to the final compounds.

Since the 1900s coumarin is well known by its pharmacological, antibacterial, anti-inflammatory, anti-coagulant, anti-oxidant and anticancer activity (O'Kennedy and Thornes 1997; Musa et al. 2008). Coumarin derivatives have a high fluorescent quantum yield being widely used as laser dyes, fluorescent probes, solar energy collector and nonlinear optical dyes (Ray and Bharadwaj 2008; Trenor et al. 2004). On the other hand, acridine chromophore is also a heterocyclic compound with great potential for the design of bio-inspired chemosensors, mostly due to their biological activities (Albert 1972). Its derivatives show a wide spectrum of biological activities, such as antibacterial (Rubbo et al. 1942), antitumor, anti-inflammatory (Amir et al. 2008; Bansal et al. 2001), hypertensive (Albert 1972), antineoplastic (Cain and Atwell 1974), analeptic (Albert 1966) and anthelmintic (Chandler and Read 1961). Acridine-based drugs are often used as photosensitizers in photodynamic therapy (PDT), which is an emerging modality in the treatment of cancer. 9-Aminoacridine also has mutagenic properties, it has the ability to bind to the DNA, and it can be used as a pH-probe in biological systems. Furthermore, it is one of the simplest organic molecules, which interact with biomolecules (Martínez and Chacón-García 2005).

The research on this kind of bioorganic molecules has allowed the detection of metal ions, and it also made it possible to quantify their amount in the human body, as well as in environmental samples.

Moreover, in order to explore the photophysical properties of organic dyes, lanthanide(III) ions have being used in conjugation with organic molecules, playing an important role in cellular imaging. Lanthanide complexes have already been used commercially in heterogeneous and homogeneous immunoassays and in DNA assays as highly sensitive and selective molecular probes (Steinkamp and Karst 2004; Hemmila and Laitala 2005). Especially, europium(III) and terbium(III) probes usually bind into an organic chelating ligand which contains a chromophore that signals the recognition. The use of luminescent lanthanide complexes has several advantages; in addition to large Stokes shift (>150 nm), their emission spectra shows very narrow bands, which are insensitive to environmental changes, long luminescent lifetimes and insensibility to photo bleaching which permits a prolonged detection (Thibon and Pierre 2009; Rajapakse et al. 2009).

Following our research interest in the design and synthesis of new colorimetric and fluorimetric probes, herein we report the synthesis of two new bio-inspired compounds (Lodeiro et al. 2010), **L1** and **L2**, containing as chromophores coumarin and/or acridine, bearing as a building block an amino acid alanine residue. Both compounds were fully characterized and their sensing ability towards different representative biological metal ions such as alkaline earth ($M = Ca^{2+}$), transition and post-transition ($M = Zn^{2+}$, Cd^{2+}, Cu^{2+}, Cr^{3+}, Fe^{3+}or Al^{3+}) metal ions was performed by UV–vis and emission fluorescence measurements. The interaction of compound **L2** with lanthanide ions ($M = Eu^{3+}$ and Tb^{3+}) was also carried out in the presence and in the absence of liposomes as potential bio-probe, as the preliminary stage to their uses as fluorescent water-soluble probes in cells and tissues.

Experimental

Chemicals and starting materials

$Zn(CF_3SO_3)_2{\cdot}xH_2O$, $Ca(CF_3SO_3){\cdot}xH_2O$, $Cd(CF_3SO_3)_2{\cdot}xH_2O$, $Cu(CF_3SO_3)_2{\cdot}xH_2O$, $Fe(NO_3)_3{\cdot}xH_2O$, $Al(NO_3)_3{\cdot}xH_2O$, $Cr(NO_3)_3{\cdot}xH_2O$, $Eu(NO_3)_3{\cdot}xH_2O$ and $Tb(NO_3)_3{\cdot}xH_2O$ salts have been purchased from Strem Chemicals, Sigma Aldrich and Solchemar. Tetrabutylammonium hydroxide ($C_{16}H_{37}NO$) and methanesulfonic acid (CH_4O_3S) were from Fluka. Thionyl chloride, DCC (*N*,*N*′-dicyclohexylcarbodiimide), Boc-Ala-OH, acridine yellow, coumarin-3-carboxylic acid were from Aldrich. HOBT (1-hydroxybenzotriazole) was from Seen Chemicals. L-Alpha-phosphatidylcholine and phosphate-buffered saline pH 7.4 were from Sigma. TLC analysis was carried out on pre-coated silica plates from Merck (Merck $60F_{254}$). Chromatography on silica gel was performed on Merck Kieselgel (230–240 mesh). All were used without previous purification.

Physical measurements

Elemental analyses were carried out on a Fisons EA-1108 analyser at the University of Vigo Elemental Analyses Service. Infrared spectra were recorded in KBr windows using a JASCO FT/IR-410 spectrophotometer. NMR

spectra of the ligands were obtained on a Bruker Spectrometer operating at 400 MHz for ^{1}H NMR and ^{13}C NMR using the solvent peak as internal reference, using the facilities of the University of Santiago de Compostela, Spain. Melting points were determined on a Gallenkamp apparatus and are uncorrected. ESI-TOF spectra were obtained on Mass Spectrometer VG Autospec M at the CACTI-Servizo de Determinación Estructural, Proteómica e Xenómica at the University of Vigo, Spain. Absorption spectra (220–800 nm) were recorded on a JASCO 650 UV–vis spectrometer and emission spectra were recorded on a Horiba-Jovin Ibon Fluoromax 4 spectrofluorimeter. The linearity of the fluorescence emission versus concentration was checked in the concentration used (10^{-4}–10^{-6} M). A correction for the absorbed light was performed when necessary. The spectrometric characterizations and titrations were performed as follows: the stock solutions of the compounds (ca. 10^{-3} M) were prepared by dissolving an appropriate amount of the complex in a 10 ml volumetric flask and diluting it to the mark with absolute ethanol or acetonitrile. The solutions were prepared by appropriate dilution of the stock solutions still 10^{-5}–10^{-6} M. Titrations of the ligands **L1**, **L2**, and **L3** were carried out by the addition of microliter amounts of standard solutions of the ions and anions in acetonitrile. All the measurements were performed at 298 K.

Luminescence quantum yields were measured using a solution of quinine sulphate in sulphuric acid (0.5 M) as a standard (ϕ) = 0.54 for **L1,** and for **L2** were measured using as standard the acridine yellow G (**L3**) ($\phi = 0.47$) (Montalti et al. 2006) and the compound **L1** ($\phi = 0.02$). All fluorescent quantum yields were corrected for different refraction indexes of solvents (Montalti et al. 2006). The values were obtained using the formula below,

$$\phi = \phi_{st} \times \frac{I}{I_{st}} \times \frac{n^2}{n_{st}^2} \times \frac{A_{st}}{A}$$

where, ϕ, ϕ_{st} are the fluorescence quantum yields of the sample and standard, n, n_{st} the solvent refraction indexes, I, I_{st} the integrated emission of sample and the standard. The A and A_{st}, are the absorbance of sample and standard at the excitation wavelength, which are matched to be identical.

Fluorescence decays were measured with excitation at 370 nm using a Nano LED system consisting of a Nano LED controller (Jobin Yvon IBH NanoLED-C) and a Nano LED source (Jobin Yvon IBH NanoLED-03). The Nano LED controller NIM output signal was shaped into a leading edge discriminator (Canberra 2126) and directed to a time to amplitude converter (TAC, Canberra 2145) as start pulses. Emission wavelengths were selected by a monochromator (Oriel 77250), imaged in a fast photomultiplier (Philips XP2020Q) and the PM signal was shaped into a constant fraction discriminator (Canberra 2126) and delayed before entering the TAC as stop pulses. The analogue TAC signals were digitized (ADC, ND582) and stored in a multichannel analyser installed in a PC. Fluorescence decays and the instrumental response function (IRF) were collected using 1,024 channels in a 38 ps per channel scale, until 5×10^3 counts at maximum were reached. The full width at half-maximum of the IRF was about 1.2 ns and was highly reproducible. Fluorescence decays were collected at 406 and 492 nm. The obtained fluorescence decays were deconvoluted using the modulating functions method (Striker et al. 1999).

Liposome preparation

Phosphate-buffered saline (PBS) pH 7.4 was prepared in doubly distilled water. Liposomes were prepared by the thin layer evaporation technique. Phosphatidylcholine was dissolved in $CHCl_3$ (10 mg/ml) and the solvent was removed under reduced pressure to obtain a thin film on the sides of the flask. The film was left under vacuum overnight for the removal of all traces of the organic solvent. The resulting dried lipidic film was dispersed with 10 ml of PBS. The mixture was vortexed and sonicated to give small unilamellar vesicles (SUV).

General synthesis of ligands

L1: coumarin-alanine

L1. Coumarin-3-carboxylic acid (**A**) (0.20 g, 1.05×10^{-3} mol) was dissolved in distilled DMF (2 ml), cooled in an ice bath, followed by the addition of HOBt (0.14 g, 1.05×10^{-3} mol) and DCC (0.21 g, 1.05×10^{-3} mol). The mixture was stirred in an ice bath for 30 min.

In a separate flask, thionyl chloride (0.40 ml, 5.60×10^{-3} mol) was added drop wise and stirred to methanol (10 ml), cooled in an ice bath, followed by the addition of Boc-Ala-OH (0.50 g, 5.61×10^{-3} mol). The solution was refluxed at boiling temperature for 2 h. The solvent was evaporated under reduced pressure, yielding an oil. The oil was washed with cold diethyl ether leaving a white powder (HCl.H-Ala-OMe).

Following the next step, HCl.H-Ala-OMe (0.14 g, 1.05×10^{-3} mol) was neutralized with triethylamine (0.14 ml, 1.05×10^{-3} mol) in distilled DMF for 30 min. The solution was filtered and the filtrate was added to the previous mixture containing compound (**A**). The final mixture was stirred for 1 h in an ice bath and 1 h at room temperature. The solvent was evaporated under reduced pressure and the residue was treated with cooled acetone, to remove *N*-acylurea (DCU) through filtration. The solvent was evaporated and the residue purified by column

chromatography with silica gel (eluent: CH_2Cl_2/MeOH 100:1). The fractions were combined and the product **L1** was obtained as a yellow solid.

Yellow powder (yield: 0.202 g, 70 %), $C_{14}H_{13}NO_5$. FW = 275.26.

Elemental analysis (found: C, 61.3; H, 4.9; N, 4.7 % CHNS requires: C, 61.0; H, 4.8; N, 5.0). IR (KBr windows) cm^{-1}: *v* (NH st) (cm^{-1}) = 3,347; *v* (alkyl-CH) (cm^{-1}) = 2,937, 2,947; *v* (C=O lactone) (cm^{-1}) = 1,720; (C=O st carboxylic acid) (cm^{-1}) = 1,711; *v* (C=C benzene) (cm^{-1}) = 1,648, 1,449, 1,362, 1,286; *v* (N–C=O st) (cm^{-1}) = 1,565; *v* (C–O–C cyclic ethers) (cm^{-1}) = 1,221, 1,202. NMR spectrum: δ_H ($CDCl_3$, 400 MHz) ppm: 1.49–1.52 (d, J = 12 Hz, 3H, β-CH_3 Ala), 3.74 (s, 3H, OCH_3), 4.70–4.73 (m, 1H, α-H Ala), 7.32–7.38 (m, 2H, H6, H7), 7.60–7.65 (m, 2H, H5, H8), 8.84 (s, 1H, H3), 9.17–9.19 (d, J = 8 Hz, 1H, NH Ala). δ_C ($CDCl_3$, 100 MHz) ppm: 18.00 (C–β-CH_3), 48.63 (αC), 52.45 (OCH_3), 116.64 (C6), 125.25 (C7), 129.80 (C5), 134.16 (C8), 148.56 (C3), 154.48 (C=O amide carbonyl). UV–vis in absolute ethanol (λ nm), bands at 295 nm ($\log\varepsilon$ = 4.0), 330 nm ($\log\varepsilon$ = 3.75). Emission spectra in absolute ethanol (λ_{exc} = 330 nm, λ_{emis} = 410 nm). ESI-TOF calc. (found) %: [**L1**]H^+, 276.3 (276.5) 100 % *m/z*.

L2: coumarin-alanine-acridine-alanine-coumarin

Coumarin-alanine (**L1**), (0.060 g, 2.18 × 10^{-4} mol) was dissolved in 1,4-dioxane (1 ml) in an ice bath, and aqueous sodium hydroxide 1 M solution (0.32 ml, 1.5 eq., 3.27 × 10^{-4} M) was added drop wise. The mixture was stirred at room temperature for 3 h. The pH was adjusted to 2–3 by adding aqueous $KHSO_4$ 1 M solution and extracting it with ethyl acetate (3 × 10 ml). After drying it with anhydrous sodium sulphate and the evaporation of the solvent, the residue was triturated with diethyl ether and a white solid (**B**, coumarin-alanine-OH) was obtained.

Compound **B** (0.054 g, 2.06 × 10^{-4} mol) was dissolved in distilled DMF (2 ml), cooled in an ice bath, followed by the addition of HOBt (0.03 g, 2.06 × 10^{-4} mol) and DCC (0.05 g, 2.06 × 10^{-4} mol). The mixture was stirred in an ice bath for 30 min.

Following the next step, acridine yellow G (**L3**) (0.056 g, 2.06 × 10^{-4} mol) was added to the solution containing compound **B** and the final mixture was stirred for 1 h in an ice bath and 1 h at room temperature. The solvent was evaporated under reduced pressure and the residue was treated with cooled acetone, to remove *N*-acylurea (DCU) through filtration. The solvent was again evaporated and the residue purified by precipitation. Product **L2** was obtained as an orange solid.

Orange powder (yield: 0.070 g, 50 %), $C_{41}H_{33}N_5O_8$ $6H_2O$, FW = 831.8.

Elemental analysis (found: C, 57.4; H, 5.6; N, 12.5 % CHNS requires: C, 57.1; H, 5.9; N, 12.2). IR (KBr windows) cm^{-1}: *v* (NH st) (cm^{-1}) = 3,030; *v* (alkyl-CH) (cm^{-1}) = 2,923, 2,847; *v* (C=O lactone) (cm^{-1}) = 1,712; (C=O st carboxylic acid) (cm^{-1}) = 1,681; *v* (C=C benzene) (cm^{-1}) = 1,622, 1,446, 1,392, 1,286; *v* (N–C=O st) (cm^{-1}) = 1,564; *v* (C–O–C cyclic ethers) (cm^{-1}) = 1,214. NMR spectrum: δ_H (C_3H_6O, 400 MHz) ppm: 1.52–1.54 (d, 6H, 2 × β-CH_3 Ala), 2.78 (s, 6H, -CH_3 acridine), 4.65–4.68 (m, 1H, α-H Ala), 7.39–7.49 (m, 4H, H6-H7, H6′-H7′), 7.52–7.56 (m, 4H, H5, H8, H5′, H8′), 7.70–7.72 (d, J = 8 Hz, 2H, 2× NH acridine), 7.77–7.81 (m, 3H, H6″, H10″, H8″), 7.92–7.98 (m, 5H, H3″ + H13″, 2× NH coumarin), 8.91 (s, 2H, H3, H3′). δ_C (C_3H_6O, 100 MHz) ppm: 17.55 (β-CH_3 Ala), 33.44 (CH_3acridine), 48.15 (αC Ala), 109.35 (C8″), 116.24 (C6, C6′), 118.72 (C6″), 119.10 (C10″), 124.38 (C7, C7′), 125.15 (C5, C5′), 127.18 (C8, C8′), 130.20 (C3″), 134.15 (C13″), 148.11 (C3, C3′). UV–vis in absolute ethanol (λ nm): bands at 295 nm ($\log\varepsilon$ = 4.45), 330 nm ($\log\varepsilon$ = 4.20), and 462 nm ($\log\varepsilon$ = 3.28). Emission spectra in absolute ethanol (λ_{exc1} = 330 nm, λ_{exc2} = 462 nm, λ_{emis1} = 410 nm, λ_{emis2} = 492 nm). ESI-TOF calc. (found) %: [**L2**] H^+ 724.5 (724.7) 100 %.

L3: acridine yellow

Acridine yellow G was a commercial product from Aldrich and used without any further purification.

Results and discussion

Synthesis

Compound **L1** was obtained by a standard DCC/HOBt coupling reaction between H-Ala-OMe and coumarin-3-carboxylic acid (A). **L1** was purified by gel chromatography yielding a yellow powder. The synthesis of compound **L2** was obtained by a reaction between compound **B** (coumarin-Ala-OH) and commercial acridine yellow G (**L3**), which was stirred for 1 h at 0 °C and 1 h at room temperature. The final product was purified by precipitation yielding an orange powder (Scheme 1).

Both compounds were characterized by elemental analysis, ^1H and ^{13}C NMR, infrared spectroscopy (KBr discs), melting point, ESI-TOF (electrospray ionization-time of flight-mass), UV–vis absorption and emission spectroscopy, fluorescence quantum yields and lifetimes.

The ^1H NMR spectra of compounds **L1** and **L2** present the characteristic signals of the amino acid backbone NH and α-H and side chain β-CH_3 (for Ala). Also, the signals, due to the heterocyclic rings, presented in coumarin and acridine moieties were visible between 7.32 and 8.91 ppm.

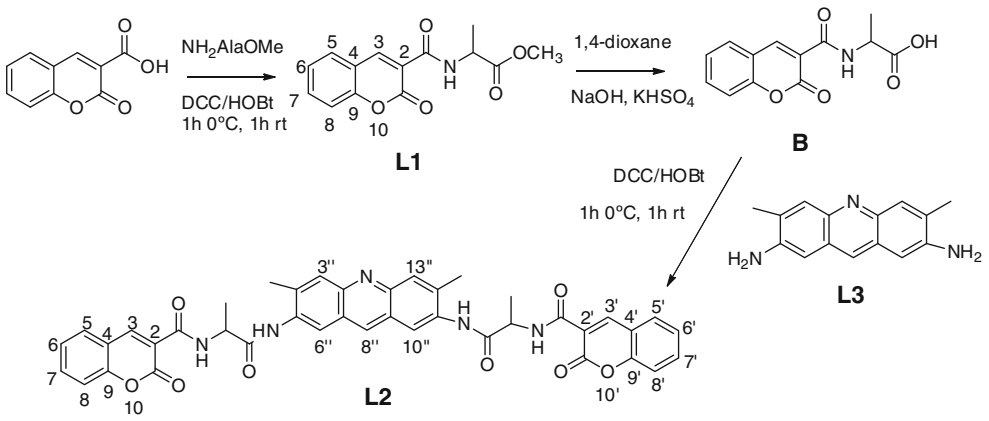

Scheme 1 General synthetic pathway of **L1** and **L2**

Through the ^{13}C spectra, the formation of the amide linkage was also confirmed by the appearance of the signal due to the amide carbonyl group at about 148 ppm as well as by the α carbon at 48.2–48.6 ppm. The IR spectra reveals some of the principal signals, such as, the N–H linkage at 3,347 cm^{-1}, carbonyl of the lactone and of the acid carboxylic at 1,720 and 1,711 cm^{-1}, respectively (Silverstein et al. 1980). Moreover, through ESI-TOF analysis it is possible to identify the protonated species [**L1**] H^+ at 276.5 *m/z* and [**L2**] H^+ at 724.7 *m/z*.

Spectrophotometric and spectrofluorimetric studies

The photophysical characterization of the compounds **L1** and **L2** was performed in acetonitrile solution and the spectra are gathered on Fig. 1. The absorption and the emission spectra shows the characteristics bands of coumarin chromophore centered at ca. 295, 330 and 406 nm for **L1** and **L2** as well as the acridine yellow characteristic bands at 290, 462 nm for absorption and 492 nm for emission in **L2**.

The relative fluorescent quantum yield of compound **L1** was calculated using as a standard the quinine sulphate, whereas for compound **L2** the fluorescent quantum yield was determined, respectively, by acridine yellow G (**L3**) and, also by the compound **L1**.

The fluorescent quantum yield of compound **L1** and **L2** is similar when it is excited on the coumarin unit, 0.02. Otherwise, on the acridine unit, compound **L2** is much more quenched, respectively, to **L3**, changing from 0.47 (**L3**) to 0.09 (**L2**). The main photophysical data are presented in Table 1.

As we can see, the fluorescent quantum yield of the acridine (**L3**) is rather quenched with the addition of the bis-coumarin-alanine moiety, changing from 0.47 to 0.09 (Montalti et al. 2006). In the emission spectrum reported in Fig. 1, compound **L2** showed a band at 410 nm and a shoulder at 492 nm, when it is excited at 330 nm, wavelength corresponding to the absorption band of the coumarin unit. Moreover, a small quenching of about 20 %, in the fluorescence quantum yield of the coumarin fluorophore of **L2** is also observed. This could be possibly due to

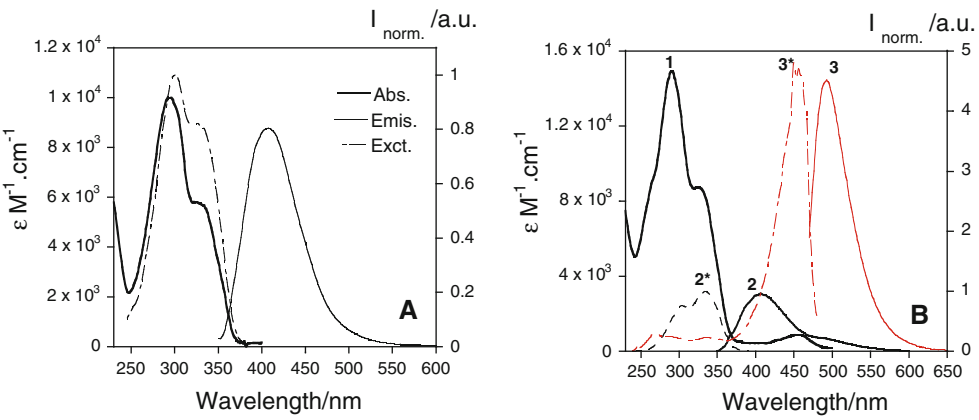

Fig. 1 **a** Absorption, emission and excitation spectra of compound **L1**. **b** Absorption (*1*), Emission at 330 nm (*2*), Emission at 462 nm (*3*), Excitation at 410 nm (*2**) and Excitation at 492 nm (*3**) spectra of compound **L2** in acetonitrile solution ($T = 298$ K, [**L1**] $= 1.27 \times 10^{-5}$ M, [**L2**] $= 7.66 \times 10^{-6}$ M, $\lambda_{excL1} = 330$ nm, $\lambda_{excL2} = 462$ and 330 nm)

Table 1 UV–vis and fluorescence data for **L1**–**L3** in acetonitrile

Compounds	UV–vis		Fluorescence		
	λ_{exc} (nm)	Log ε	λ_{em} (nm)	Stokes' shift (nm)	Quantum yield ϕ
L1	330	3.84	406	76	0.02
L2	330	3.94	406	76	0.02 (λ_{exc} = 294 nm)
	462	2.93	492	30	0.09 (λ_{exc} = 453 nm)
L3	462	3.02	492	30	0.47

low intramolecular energy transfer from the coumarin unit to the acridine.

Fluorescence decays were measured in acetonitrile with excitation at 370 nm. The fluorescence decay of compound **L1** (CoumAla), collected at 406 nm, is well fitted with a single exponential law, with a decay time of 0.25 ns. The fluorescence decay of compound **L3** (acridine) collected at 492 nm is also well fitted with a single exponential law with a decay time of 4.40 ns. The fluorescence decay of **L2** was collected at 406 and 492 nm, and the global fitting is presented in Fig. 2.

At 406 nm the decay of **L2** is still fitted with a single exponential with a decay time of 0.21 ns, while at 492 nm the decay is best fitted with a sum of two exponentials. A shorter decay time identical to the one obtained at 406 nm (0.21 ns), assignable to the coumarin moiety and a longer decay time (4.37 ns) typical of the acridine moiety are observed.

The pre-exponential factor associated with the short decay time is positive and larger than the one obtained for the longer decay time at 492 nm. This is due to the significant contribution of the coumarinic chromophore emission at this wavelength.

Due to the very short time of the coumarin, the energy transfer in the system is not very efficient. The rate constant for energy transfer has to compete with the rapid intrinsic decay of the coumarin. Through the quenching in the decay time of the coumarin chromophore (from 0.25 to 0.21 ns), an energy transfer efficiency of 0.19 can be estimated, interestingly quite low for chromophores in such close contact and compatible with the 20 % quenching observed in the quantum yield determination.

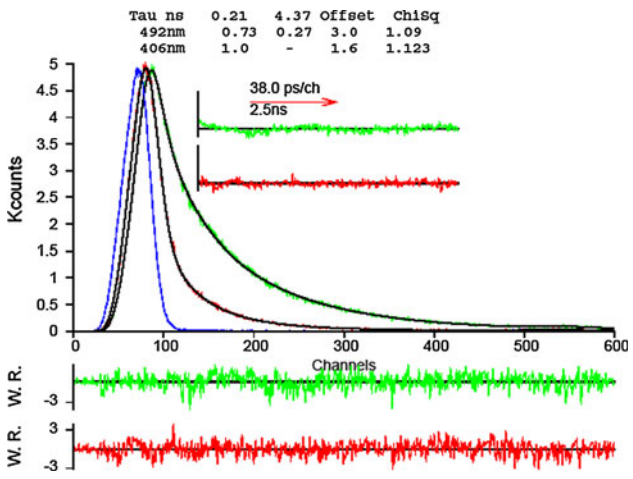

Fig. 2 Fluorescence decays and global analysis of **L2** in acetonitrile; excitation at 370 nm

The very low quantum yield observed for the acridine unit in **L2** must arise from a static quenching mechanism (ground state equilibrium between quenched and unquenched forms). The decay time obtained (4.37 ns) corresponds to the fraction of unquenched acridine. The quenched acridine fraction either does not emit or its decay time is below our experimental resolution.

In order to apply compounds **L1** and **L2** as metal ion chemosensors, several titrations with the addition of H^+, OH^-, alkaline earth (M = Ca^{2+}), transition and post-transition (M = Zn^{2+}, Cd^{2+}, Cu^{2+}, Cr^{3+}, Fe^{3+} and Al^{3+}) and lanthanide ions (M = Eu^{3+} and Tb^{3+}) were carried out by UV–vis and emission fluorescence measurements.

The addition of OH^- anion induces in ligand **L2** (Fig. 3c, d) a small decrease of the absorption bands centered at 295 and 462 nm, and a strong quenching (ca. 95 %) of the emission fluorescence at 406 and 492 nm. In order to shed more light to the system **L2**, the parent compounds **L1** and **L3** were also studied.

Compound **L1** is more affected than **L2** in the presence of a basic environment, showing a strong decrease in the absorption and emission spectra (see Fig. 3a, b) with the addition of ca. one equivalent of OH^- anion. Compound **L3** shows a decrease and a blue shift, from 462 to 410 nm, in the absorbance as well as a quenching in the emission intensity at 492 nm (data not shown). The quenching of the emission presented for the **L1**, **L2** and **L3** systems after the anion addition, is probably due to the deprotonation in the nitrogen atoms in the alanine amino acid, leaving a lone pair of electrons available, allowing photoinduced electron transfer (PET) to occur (Lodeiro and Pina 2009; Tamayo et al. 2005; Lodeiro et al. 2006; Oliveira et al. 2011a, b). This result is in agreement with other systems studied previously in our group based on amino acids or polyamine (Costa et al. 2007; Albelda et al. 2002). On the contrary, compounds **L1** to **L3** do not show any changes in an acidic environment.

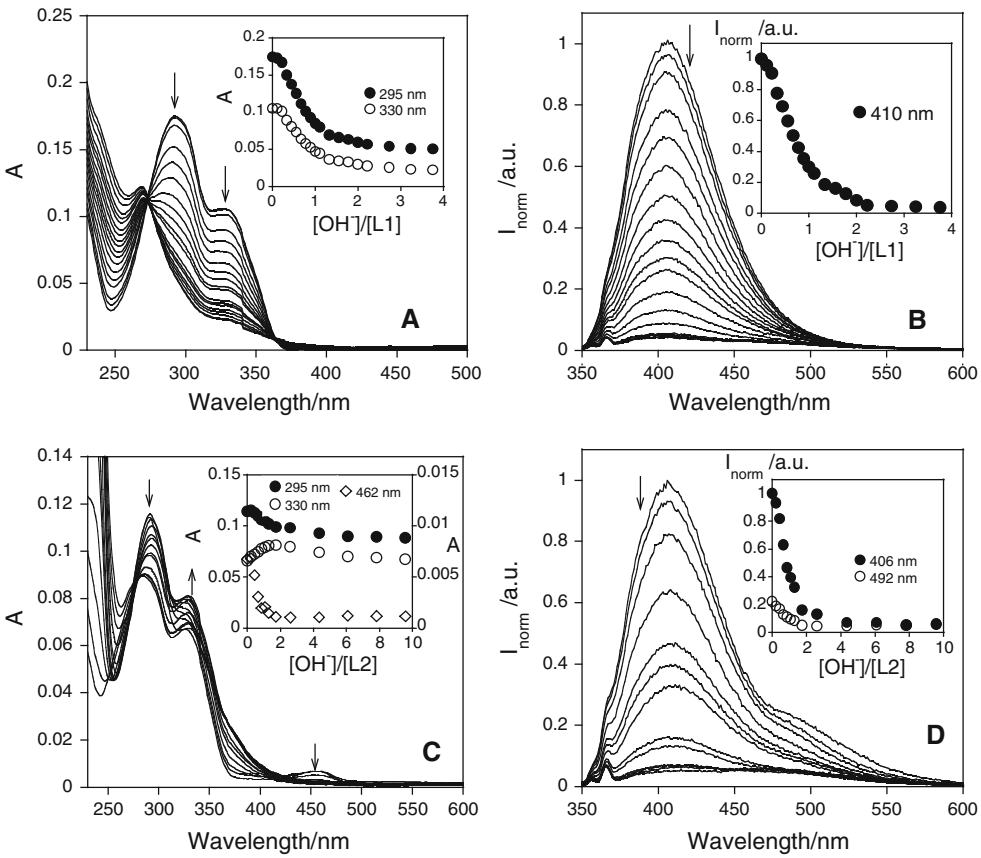

Fig. 3 Spectrophotometric (**a**, **c**) and spectrofluorimetric (**b**, **d**) titration of compounds **L1** (**a** and **b**) and **L2** (**c** and **d**) with the increasing amount of OH^- anion in acetonitrile solution. [**L1**] = 1.27×10^{-5} M, [**L2**] = 7.66×10^{-6} M $\lambda_{excL1=L2} = 330$ nm, $T = 298$ K

Interaction with alkaline earth (M = Ca^{2+}), transition and post-transition (M = Zn^{2+}, Cd^{2+}, Cu^{2+}, Cr^{3+}, Fe^{3+} and Al^{3+}) metal ions

Compounds **L1** and **L2** do not show spectral changes in the presence of Ca^{2+}, Zn^{2+}, Cd^{2+}, Cu^{2+}, Cr^{3+} and Al^{3+} in an pure acetonitrile solution. However, when the systems were first deprotonated, with the addition of ca. 2 equivalents of OH^-, intense changes in the absorption and emission spectra towards the mentioned metal ions were observed. For most of the transition and post-transition metal ions, a similar behaviour was observed. Figure 4 shows the absorption and emission of **L1**, **L1** deprotonated (**L1**$^-$); and **L1** deprotonated after the addition of M^{n+} (Ca^{2+}, Zn^{2+}, Cd^{2+}, Cu^{2+}, Cr^{3+}, Fe^{3+}or Al^{3+}) (**L1**$^-$**M**) metal ions as well as the spectrofluorimetric titration of **L1**$^-$ with Al^{3+} in an acetonitrile solution.

The addition of the anion OH^- induces a decrease and a blue shift on the absorbance at 330 nm followed by the quenching in the emission intensity at 410 nm. Upon interaction with the aforementioned metal ions, a recovery of the emission was observed, in addition, the absorption spectrum returns to its initial form instead of to lower absorption values.

With an exception for Ca^{2+}, Cu^{2+}, and Cr^{3+} where no recovery was observed, it is interesting to note that the stronger recovery was observed with Al^{3+} interaction with four times enhancement in the emission intensity (see Fig. 4b), followed by Zn^{2+}, Cd^{2+} with two times emission enhancement. So, due to the absorption and emission spectra changes we could conclude that probably, after the deprotonation on the amide group, the metal ions coordinate with the molecule involving the alanine and the lactone from the coumarin ring (see Fig. 6). However, the higher size and charge of the metal ion in respect to the proton reveals not to be efficient enough to recover the total initial emission. On the other hand, the addition of Fe^{3+} promotes a total quenching in the emission intensity.

Figure 5 shows the absorption and emission titrations of deprotonated **L2** with Zn^{2+} and Al^{3+}.

Upon the addition of Zn^{2+} and Al^{3+} metal ions an increase in the fluorescence emission was observed, contrary to the effect detected by Fe^{3+}, in which a total quenching in the emission intensity has occurred. In the absorption spectra, a decrease at 330 nm and an increase at 462 nm in the absorption were observed, followed by the enhancement of the emission intensity at 406 and 492 nm. In both cases, with the addition of Zn^{2+} and Al^{3+}, a total recovery of the **L2** emission was verified. Metal ion coordination in **L2** probably takes place by the alanine amino acid and the lactone of the coumarin ring. Complexation involved the electron lone pairs of nitrogen present in the

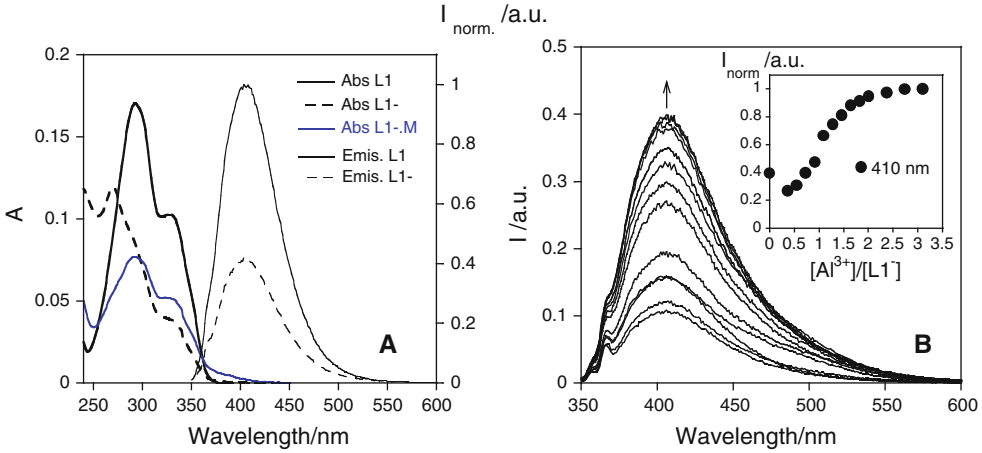

Fig. 4 Absorption and emission spectra **a** of compounds **L1**, $\mathbf{L1}^-$ and $\mathbf{L1}^-$.M, M = Ca^{2+}, Zn^{2+}, Cd^{2+}, Cu^{2+}, Cr^{3+}, Fe^{3+}or Al^{3+}; and **b** spectrofluorimetric titration of $\mathbf{L1}^-$ in the increasing amount of Al^{3+} in an acetonitrile solution (T = 298 K, [**L1**] = 1.27 × 10^{-5} M, λ_{exc} = 330 nm)

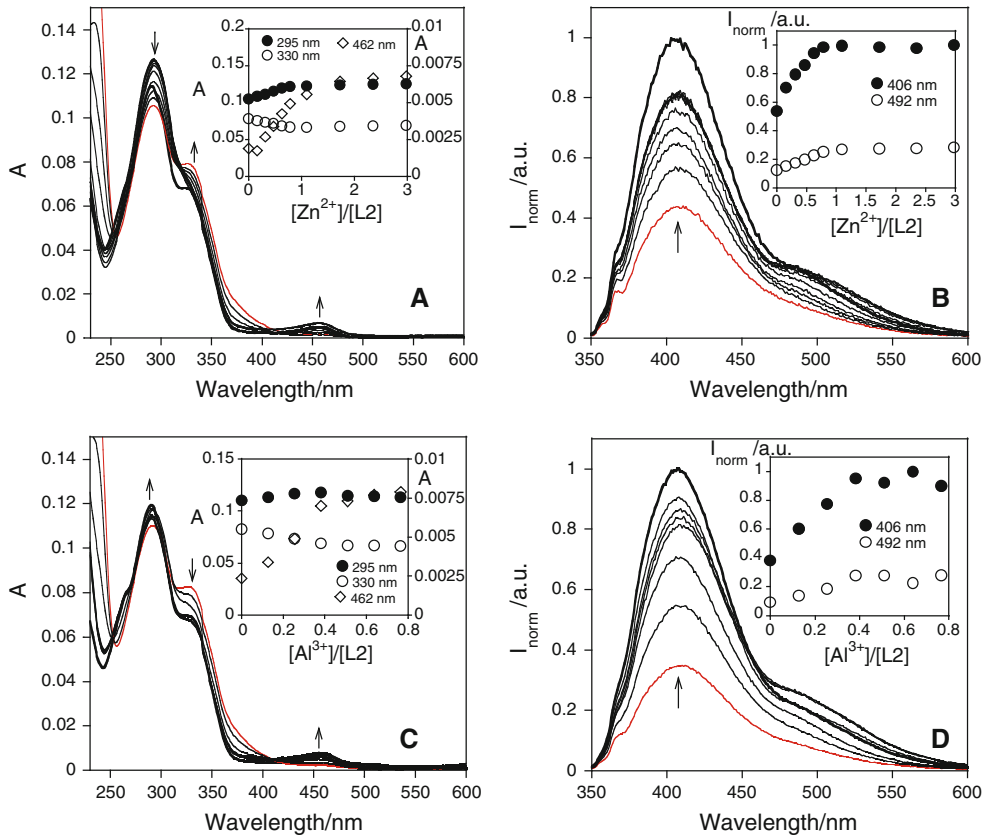

Fig. 5 Spectrophotometric and spectrofluorimetric titrations of compound **L2** deprotonated with the addition of Zn^{2+} (**a**, **b**), and Al^{3+} (**c** and **d**) in acetonitrile. The *inset* (**a**, **c**) shows the absorbance as a function of [Zn^{2+}]/[**L2**] (**a**), [Al^{3+}]/[**L2**] (**c**) at 295, 330 and 462 nm; the *inset* (**b**, **d**) shows the emission as a function of [Zn^{2+}]/[**L2**] (**b**), [Al^{3+}]/[**L2**] (**d**) at 406 and 492 nm. ([**L2**] = 7.66 × 10^{-6} M, T = 298 K, λ_{exc} = 330 nm)

molecule, which blocks the PET phenomena. With Ca^{2+}, Cu^{2+} and Cr^{3+} no spectral changes were observed.

The association constants for Zn^{2+}, Cd^{2+} and Al^{3+} interaction were determined using a HypSpec (Gans et al. 1996) program (Table 2). For **L1** a complex formed by two units of **L1** by one metal ion was postulated (see Fig. 6), with a constant of $\log K_{ass}Al^{3+} = 7.663 \pm 0.052 > \log K_{ass}Cd^{2+} = 3.654 \pm 0.033 > \log K_{ass}Zn^{2+} = 3.095 \pm 0.033$.

In the case of compound **L2**, two units per Al^{3+} were determined, with a constant of $\log K_{ass}Al^{3+} = 9.949 \pm 0.022$. However, in the cases of Zn^{2+} and Cd^{2+} a mononuclear complex (1:1) was observed with a constant of

Table 2 Association constants $\log K_{ass}$ with compounds **L1** and **L2** in acetonitrile obtained by Hypspec program

Compounds	L1	L2
Zn^{2+}	3.095 ± 0.033 (2:1)	7.995 ± 0.061 (1:1)
Cd^{2+}	3.654 ± 0.033 (2:1)	7.405 ± 0.027 (1:1)
Al^{3+}	7.663 ± 0.052 (2:1)	9.949 ± 0.022 (2:1)
Eu^{3+}	–	11.689 ± 0.010 (3:2)
Tb^{3+}	–	16.559 ± 0.010 (3:2)

(1:1) = LM, (2:1) = L_2M, (3:2) = L_3M_2

$\log K_{ass}Zn^{2+} = 7.995 \pm 0.061 > \log K_{ass}Cd^{2+} = 7.405 \pm 0.027$; this being the most stable interaction observed with aluminium (III) (see Fig. 6).

These results suggest that compound **L2** can be used as fluorescent non-natural amino acid fluorescent probe for the detection of Zn^{2+}, Cd^{2+} and Al^{3+}.

Eu^{3+} and Tb^{3+} titrations and their interaction in liposomes

Recent efforts have been made in the development of luminescent lanthanide complexes as responsive probes for live-cell imaging applications. Europium(III) and terbium(III) are often incorporated into an organic part of the ligand in order to study internal energy transfer processes. The fluorophore acts as antenna to the lanthanide ion present in the complex. When the fluorophore is excited, an intersystem crossing the triplet state of the fluorophore occurs with a consequent intramolecular energy transfer (ET) from the fluorophore to the excited state of the lanthanide(III). As a result, emission peaks at 545, 581 and 618 nm for terbium (corresponding to the excited states $^7F_5$, $^7F_4$ and $^7F_3$) and at 578, 590 nm ($^7F_1$ transition), 614 nm ($^7F_2$ transition) and 683, 697 nm ($^7F_4$ transition) for europium are observed (see Fig. 7) (Bazzicalupi et al. 2001; Li and Wong 2002).

In order to explore the dual emission of our complexes, titrations of compound **L2** with Eu^{3+} and Tb^{3+} in acetonitrile were performed.

As can be seen in Fig. 7a, b, the intramolecular energy transfer from **L2** to the Eu^{3+} and Tb^{3+} is quite efficient, with an intense increase in the emission at 578, 590, 614, 683 and 697 nm for Eu^{3+} and at 542, 581 and 618 nm for Tb^{3+}. Although, the energy transfer from ligand to metal was not total since the emission band of the ligand remains in the spectrum (see Fig. 8) the naked-eye detection, under a UV lamp, of both metals is possible due to the interesting pink-orange (Eu^{3+}) and green (Tb^{3+}) colour observed. Using the HypSpec program the association constant of the lanthanide(III) complexes, $\log K_{ass}Tb^{3+} = 16.559 \pm 0.010 > \log K_{ass}Eu^{2+} = 11.689 \pm 0.010$ was determined, with a stoichiometry in both cases of three ligands per two metal ions (see Fig. 8).

Finally, with the aim of solubilized **L2** as a more complex structure in cells and water environments for energy transfer studies, titrations with Eu^{3+} and Tb^{3+} in acetonitrile in the presence of liposomes prepared in a PBS solution were performed (Marchi-Artzner et al. 2004).

In the presence of liposomes the lanthanide(III) emission bands were reduced in intensity when compared with the previous results in pure acetonitrile, suggesting a lower ligand-to-metal energy transfer. This result points out that some water molecules from the liposomes could be interacting with the coordination sphere of the lanthanide(III) ions (Bazzicalupi et al. 2001; Roy et al. 2000). However, the appearance of the red and green colour still occurs (see Fig. 7c, d). This partial water quenching could be overcome incorporating $(\mathbf{L2})_3(Ln^{3+})_2$ complex inside silica shell nanoparticles. This kind of strategy allows the protection of the liposomes from water molecules and oxygen, which are the most potential quenchers of the emission signal (Folliet et al. 2011).

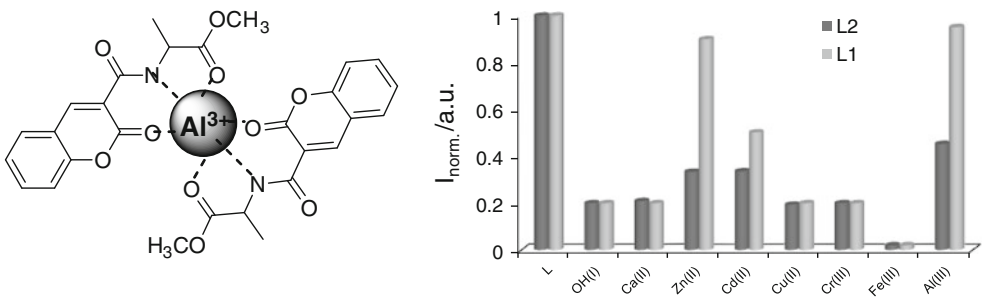

Fig. 6 *Left* mechanism proposed for the aluminium metal ions coordination to **L1** and *right* normalized emission of compounds **L1** and **L2**, deprotonated, and deprotonated in the presence of Ca^{2+}, Zn^{2+}, Cd^{2+}, Cu^{2+}, Cr^{3+}, Fe^{3+}or Al^{3+} metal ions

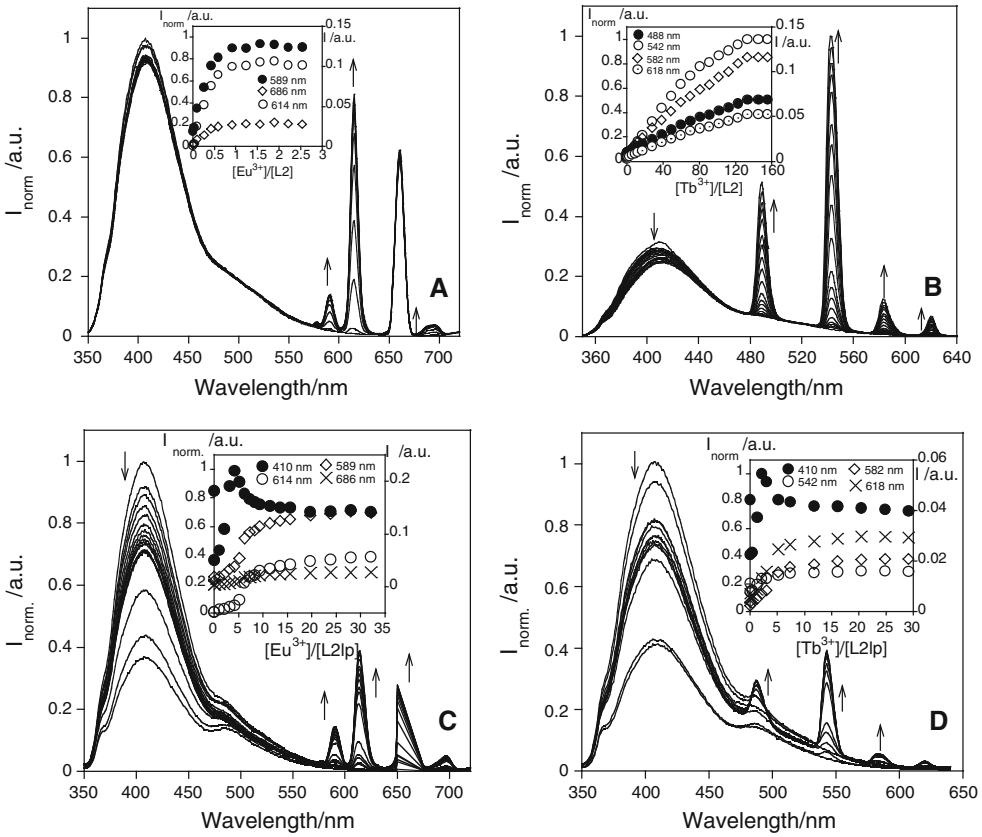

Fig. 7 Spectrofluorimetric titration of **L2** (**a**, **b**), and **L2** with liposomes (addition of 30 µl) (**c**, **d**) in the increasing addition of Tb^{3+} (**b**, **d**) and Eu^{3+} (**a**, **c**) in acetonitrile. [**L2**] = 7.66 × 10^{-6} M, λ_{exc} = 330 nm, T = 298 K)

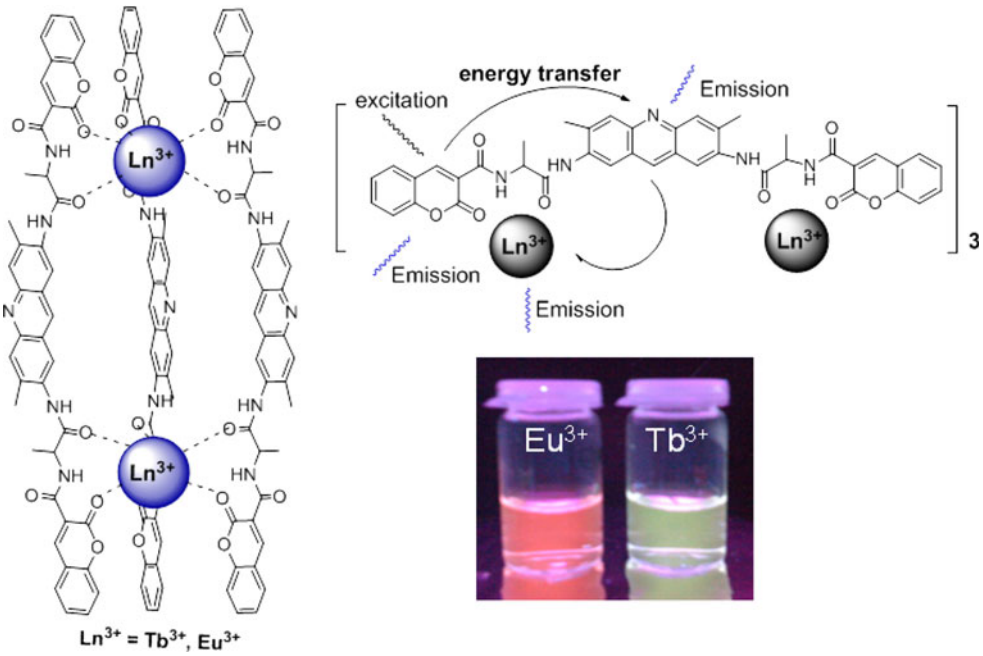

Fig. 8 Schematic representation of compound **L2** in the presence of Eu^{3+} and Tb^{3+} ions and image of the solution of **L2** Tb^{3+} (*green emission*) and **L2** Eu^{3+} (*orange-pink emission*) under UV lamp, λ_{exc} = 365 nm (colour figure online)

Conclusions

Two new bio-inspired compounds **L1** and **L2** containing coumarin and/or acridine as chromophores and bearing an alanine amino acid as spacer were successfully synthesized and well characterized. Both compounds appeared be very sensitive in a basic environment attributed to the photoinduced electronic transfer phenomena (PET). After the addition of Zn^{2+}, Cd^{2+} and Al^{3+} metal ions, compounds **L1** and **L2** in their deprotonated form show an important

recovery of the emission intensity. In both cases, the most stable metal complex formed was obtained with Al^{3+} with an association constant of $\log K_{ass}$ of 7.663 ± 0.052 (**L1**) and 9.949 ± 0.022 (**L2**).

In order to obtain luminescent complexes in the electromagnetic visible spectrum, titration of **L2** with the lanthanide ions Eu^{3+} and Tb^{3+} was also performed with and without liposomes. In both cases an interesting pink-orange (Eu^{3+}) and green (Tb^{3+}) emissive colours were observed. However, in liposomal water environment a lower energy transfer from ligand to metal was observed, with a significant reduction of the fluorescence quantum yield of the metal ion. In order to prevent this partial water quenching and overcome this disadvantage, studies of $(\mathbf{L2})_3(Ln^{3+})_2$ species incorporating $(\mathbf{L2})_3(Ln^{3+})_2$ complex inside silica shell nanoparticles are in progress.

Acknowledgments We are indebted to Xunta de Galiza (Spain) for projects 09CSA043383PR and 10CSA383009PR in biomedicine, and the Scientific Association ProteoMass for financial support. E.O. thanks the FCT-MEC (Portugal) for the Postdoctoral grant SFRH/BPD/72557/2010. J.L.C. and C.L. thank to Xunta de Galicia (Spain) for the Isidro Parga Pongal research contracts.

Conflict of interest The authors declare that they have no conflict of interest.

References

Albelda MT, Diaz P, Garcia-España E, Lima JC, Lodeiro C, de Melo JS, Parola AJ, Pina F, Soriano C (2002) Switching from intramolecular energy transfer to intramolecular electron transfer by the action of pH and Zn^{2+} co-ordination. Chem Phys Lett 353:63–68

Albert A (1966) In: The acridines: their preparation, physical, chemical, and biological properties and uses, 2nd edn. Edward Arnold, London

Albert A (1972) Medicinal chemical monograph. In: Ariens EJ (ed) Drug design, vol 3. Academic Press, New York

Amir M, Kumar H, Khan SA (2008) Synthesis and pharmacological evaluation of pyrazoline derivatives as new anti-inflammatory and analgesic agents. Bioorg Med Chem Lett 18:918–922

Bansal E, Srivastava VK, Kumar A (2001) Synthesis and anti-inflammatory activity of 1-acetyl-5-substituted aryl-3-(beta-aminonaphthyl)-2-pyrazolines and beta-(substituted aminoethyl) amidonaphthalenes. Eur J Med Chem 36:81–92

Bazzicalupi C, Bencini A, Berni E, Bianchi A, Giorgi C, Valtancoli B, Lodeiro C, Roque A, Pina F (2001) Coordination properties of a polyamine cryptand with two different binding moieties. A case of a pH-modulated antenna device based on a new Eu(III) cryptate complex. Inorg Chem 40:6172–6179

Burdette SC, Walkup GK, Spingler B, Tsien RY, Lippard SJ (2001) Fluorescent sensors for Zn^{2+} based on a fluorescein platform: synthesis, properties and intracellular distribution. J Am Chem Soc 123:7831–7841

Cain BF, Atwell GJ (1974) The experimental antitumour properties of three congeners of the acridylmethanesulphonanilide (AMSA) series. Eur J Cancer 10:539–547

Chandler A, Read C (1961) Introduction to parasitology, 10th edn. Wiley, New York

Costa SPG, Oliveira E, Lodeiro C, Raposo MMM (2007) Synthesis, characterization and metal ion detection of novel fluoroionophores based on heterocyclic substituted alanines. Sensors 7:2096–2114

Costa SPG, Oliveira E, Lodeiro C, Raposo MMM (2008) Heteroaromatic alanine derivatives bearing (oligo)thiophene units: synthesis and photophysical properties. Tetrahedron Lett 49:5258–5261

Folliet N, Roiland C, Bégu S, Aubert A, Mineva T, Goursot A, Selvaraj K, Duma L, Tielens F, Mauri F, Laurent G, Bonhomme C, Gervais C, Babonneau F, Azaïs T (2011) Investigation of the interface in silica-encapsulated liposomes by combining solid state NMR and first principles calculations. J Am Chem Soc 133:16815–16827

Gans P, Sabatini A, Vacca A (1996) Investigation of equilibria in solution. Determination of equilibrium constants with the HYPERQUAQ suite of programs. Talanta 43:1739–1753

Hemmila I, Laitala V (2005) Progress in lanthanides as luminescent probes. J Fluoresc 15:529–542

Ko SK, Yang YK, Tae J, Shin I (2006) In vivo monitoring of mercury ions using a rhodamine-based molecular probe. J Am Chem Soc 128:14150–14155

Kubo K, Mori A (2005) PET fluoroionophores for Zn^{2+} and Cu^{2+}: complexation and fluorescence behavior of anthracene derivatives having diethylamine, *N*-methylpiperazine and *N*,*N*-bis(2-picolyl)amine units. J Mater Chem 15:2902–2907

Lee HN, Kim HN, Swamy KMK, Park MS, Kim J, Lee H, Lee KH, Park S, Yoom J (2008) New acridine derivatives bearing immobilized azacrown or azathiacrown ligand as fluorescent chemosensors for Hg^{2+} and Cd^{2+}. Tetrahedron Lett 49:1261–1265

Li C, Wong W-T (2002) Luminescent terbium (III) complexes with pendant crown ethers responding to alkali metal ions and aromatic antennae in aqueous solution. Chem Commun 2034–2035

Lim NC, Bruchner C (2004) DPA-substituted coumarins as chemosensors for zinc(II): modulation of the chemosensory characteristics by variation of the position of the chelate on the coumarin. Chem Commun 9:1094–1095

Lodeiro C, Pina F (2009) Luminescent and chromogenic molecular probes based on polyamines and related compounds. Coord Chem Rev 253:1353–1383

Lodeiro C, Lima JC, Parola AJ, Seixas de Melo JS, Capelo JL, Covelo B, Tamayo A, Pedras B (2006) Intramolecular excimer formation and sensing behavior of new fluorimetric probes and their interactions with metal cations and barbituric acids. Sens Act B Chem 115:276–286

Lodeiro C, Capelo JL, Mejuto JC, Oliveira E, Santos HM, Pedras B, Nuñez C (2010) Light and colour as analytical detection tools: a journey into the periodic table using polyamines to bio-inspired systems as chemosensors. Chem Soc Rev 39:2948–2976

Lu C, Zu ZC, Cui JN, Zhang R, Qian XH (2007) Ratiometric and highly selective fluorescent sensor for cadmium under physiological pH range: a new strategy to discriminate cadmium from zinc. J Org Chem 72:3554–3557

Marchi-Artzner V, Brienne MJ, Gulik-Krzywicki T, Dedieu JC, Lehn JM (2004) Selective complexation and transport of europium at the interface of vesicles. Chemistry 10:2342–2350

Martínez R, Chacón-García L (2005) The search of DNA-intercalators as antitumoral drugs: what it worked and what did not work. Curr Med Chem 12:127–151

Montalti M, Credi A, Prodi L, Gandolfi MT (2006) Handbook of photochemistry, 3rd edn. Taylor and Francis, Boca Raton

Musa MA, Cooperwood JS, Khan MOF (2008) A review of coumarin derivatives in pharmacotherapy of breast cancer. Curr Med Chem 15:2664–2679

Nolan EM, Jaworsky J, Racine ME, Sheng M, Lippard SJ (2006) Midrange affinity fluorescent Zn(II) sensors of the Zinpyr

family: syntheses, characterization, and biological imaging applications. Inorg Chem 45:9748–9757
O'Kennedy R, Thornes RD (eds) (1997) Coumarins. Biology, applications and mode of action. Wiley, Chichester
Oliveira E, Genovese D, Juris R, Zaccheroni N, Capelo JL, Raposo MMM, Costa SPG, Prodi L, Lodeiro C (2011a) Bioinspired systems for metal-ion sensing: new emissive peptide probes based on benzo[d]oxazole derivatives and their gold and silica nanoparticles. Inorg Chem 50:8834–8849
Oliveira E, Nuñez C, Rodríguez-González B, Capelo JL, Lodeiro C (2011b) Novel small stable gold nanoparticles bearing fluorescent cysteine-coumarin probes as new metal-modulated chemosensors. Inorg Chem 50:8797–8807
Oliveira E, Nunes-Miranda JD, Santos HM (2012a) From colorimetric chemosensors to metal nanoparticles using two new tyrosine Schiff-base ligands for Cu^{2+} detection. Inorg Chim Acta 380:22–30
Oliveira E, Santos HM, Capelo JL, Lodeiro C (2012b) New emissive dopamine derivatives as fluorescent chemosensors for metal ions: a CHEF effect for Al(III) interaction. Inorg Chim Acta 381:203–211
Pazos E, Vázquez O, Mascareñas JL, Vázquez ME (2009) Peptide-based fluorescent biosensors. Chem Soc Rev 38:3348–3359
Rajapakse HE, Reddy DR, Mohandessi S, Butlin NG, Miller LW (2009) Luminescent terbium protein labels for time-resolved microscopy and screening. Angew Chem Int Ed 48:4990–4992
Ray D, Bharadwaj PK (2008) A coumarin-derived fluorescence probe selective for magnesium. Inorg Chem 47:2252–2254
Roy BD, AbulFazal MD, Arruda A, Mallik S, Campiglia AD (2000) Polymerized fluorescent liposomes incorporating lanthanide ions. Org Lett 2:3067–3070
Rubbo SD, Albert A, Maxwell MB (1942) The influence of chemical constitution on antiseptic activity I. A study of the mono-amino-acridines. J Exp Pathol 23:69–83
Silverstein RM, Bassler GC, Morrill TC (1980) Spectrometric identification of organic compounds, 4th edn. Wiley
Soh JH, Swamy KMK, Kim SK, Kim S, Lee SH, Yoon J (2007) Rhodamine urea derivatives as fluorescent chemosensors for Hg^{2+}. Tetrahedron Lett 48:5966–5969
Steinkamp T, Karst U (2004) Detection strategies for bioassays based on luminescent lanthanide complexes and signal amplification. Anal Bioanal Chem 380:24–30
Striker G, Subramaniam V, Seidel CAM, Volkmer A (1999) Photochromicity and fluorescence lifetime of green fluorescent protein. J Phys Chem B 103:8612–8617
Tamayo A, Lodeiro C, Escriche L, Casabo J, Covelo B, González P (2005) New fluorescence PET systems based on N(2)S(2) pyridine-anthracene-containing macrocyclic ligands. Spectrophotometric, spectrofluorometric, and metal ion binding studies. Inorg Chem 22:8105–8115
Thibon A, Pierre VC (2009) Principles of responsive lanthanide-based luminescent probes for cellular imaging. Anal Bioanal Chem 394:107–120
Trenor SR, Shultz AR, Love BJ, Long TE (2004) Coumarins in polymers: from light harvesting to photo-cross-linkable tissue scaffolds. Chem Rev 104:3059–3077
Yang JS, Lin CS, Hwang CY (2001) Cu^{2+}-induced blue shift of the pyrene excimer emission: a new signal transduction mode of pyrene probes. Org Lett 6:889–892
Zhang WS, Tang B, Liu X, Liu YY, Xu KH, Ma JP, Tong LL, Yang GW (2009) A highly sensitive acidic pH fluorescent probe and its application to HepG2 cells. Analyst 134:367–371